

# Modulational instability and dynamics of rational soliton solutions for the coupled Volterra lattice equation associated with $4 \times 4$ Lax pair

NAN LIU and XIAO-YONG WEN<sup>✉</sup>\*

School of Applied Science, Beijing Information Science and Technology University, Beijing 100192, China

\*Corresponding author. E-mail: xiaoyongwen@163.com

MS received 13 August 2018; revised 18 November 2018; accepted 4 January 2019; published online 21 May 2019

**Abstract.** The coupled Volterra lattice equation associated with  $4 \times 4$  Lax pair is under investigation, which is an integrable discrete form of a coupled KdV equation applied widely in fluids, Bose–Einstein condensation and atmospheric dynamics. First, we explore the conditions for modulational instability (MI) of the constant seed background for this equation. Secondly, we present the discrete Darboux transformation (DT) and generalised DT based on the new  $4 \times 4$  Lax pair. Through the resulting discrete DT, the bell-shaped and anti- $N$ -shaped soliton solutions of the coupled Volterra lattice equation are derived. Moreover, we derive the  $M$ -shaped and  $N$ -shaped rational solitons and bell-shaped and  $N$ -shaped semirational soliton solutions of the coupled Volterra lattice equation via the discrete generalised DT. Finally, we numerically study the dynamical behaviours of such soliton solutions and find that the rational and semirational soliton solutions have better numerical stability than the usual soliton solution, although three types of solutions are robust against a small noise. The results may be helpful for understanding the two-layered fluid waves near ocean shores described by the coupled Korteweg–de Vries (KdV) equation.

**Keywords.** The coupled Volterra lattice equation; modulational instability; discrete Darboux transformation; rational soliton solution.

**PACS Nos** 02.30.Jr; 05.45.Yv

## 1. Introduction

Nonlinear partial differential equations (NPDEs) may describe many physical phenomena (see refs [1–11] and references therein). Explicit exact solutions, especially soliton solutions, of the NPDEs are used for depicting and explaining such nonlinear phenomena. Very recently, there has been an increasing interest in studying the nonlinear lattice equations (NLEs) which are treated as spatially discrete analogues of NPDEs. The NLEs can be used to describe some physical phenomena such as nonlinear optics, plasma physics, electric field, population dynamics, etc. [12–17]. To understand such nonlinear phenomena described by the NLEs, searching for the explicit exact solutions of NLEs is of great theoretical significance. Some methods such as the inverse scattering transformation [17–19], the Hirota technique [20], the algebra-geometric method [21], the Darboux transformation (DT) [22–36], etc. for constructing explicit exact solutions of NLEs have

been proposed and developed. Among them, the DT based on Lax pair is a powerful approach for studying explicit exact solutions of integrable NLEs in the soliton theory and integrable systems. However, for the Lax integrable NLEs, more research is focussed on the discrete  $2 \times 2$  and  $3 \times 3$  Lax pairs in matrix form [22–33], while for the discrete  $4 \times 4$  or higher-order Lax pairs in matrix form, the relevant research is not satisfactory due to their complexity [34–36]. So, it is very meaningful to do further research on the discrete  $4 \times 4$  matrix spectral problems. In the present paper, aiming at how to construct exact solutions of an integrable NLE associated with a discrete  $4 \times 4$  Lax pair via our proposed generalised DT, we consider the following coupled Volterra lattice equation associated with  $4 \times 4$  Lax pair [37]:

$$\begin{aligned} u_{n,t} - (u_{n+1} - u_{n-1})u_n + (v_{n+1} - v_{n-1})v_n &= 0, \\ v_{n,t} - (u_{n+1} - u_{n-1})v_n - (v_{n+1} - v_{n-1})u_n &= 0. \end{aligned} \quad (1)$$

We remark here that under transformations  $u_n = -n$ ,  $v_n \rightarrow \sqrt{-\alpha}b_n$  (when  $\alpha < 0$ ), or  $v_n \rightarrow -i\sqrt{\alpha}b_n$  (when  $\alpha > 0$ ), eq. (1) changes to

$$\begin{aligned} a_{n,t} + (a_{n+1} - a_{n-1})a_n - (b_{n+1} - b_{n-1})\alpha b_n &= 0, \\ b_{n,t} + (a_{n+1} - a_{n-1})b_n + (b_{n+1} - b_{n-1})a_n &= 0, \end{aligned} \quad (2)$$

through the continuous limit

$$\begin{aligned} a_n &= 1 + \delta^2 p \left( (n - 2t)\delta, \frac{1}{3}\delta^3 t \right), \\ b_n &= \delta^2 q \left( (n - 2t)\delta, \frac{1}{3}\delta^3 t \right). \end{aligned} \quad (3)$$

Equation (2) can be reduced to a two-coupled KdV system

$$\begin{aligned} p_t + 6\alpha q q_x + 6pp_x + p_{xxx} &= 0, \\ q_t + 6qp_x + 6pq_x + q_{xxx} &= 0, \end{aligned} \quad (4)$$

which can model the two-layered fluid waves near ocean shores [38] and also is applied widely in fluids, Bose–Einstein condensation and atmospheric dynamics [39]. It is pointed out that the motivation for investigating the NLEs is their possible application to the numerical simulation, and they can maintain certain properties of the original NPDEs [40]. Therefore, as a discrete version of (4), eq. (1) or (2) may be used to explain the above-mentioned physical phenomena described by the two-coupled KdV system. In ref. [37], various explicit solutions of eq. (2), such as solitary wave, positon and complexiton, have been constructed by using a simple function expansion method. In ref. [39], eq. (1) is studied with the help of Lie point symmetries. Two types of delayed differential reduction systems are derived from eq. (1) by means of the symmetry reduction approach and symbolic computation, and some cnoidal wave and solitary wave solutions for eq. (1) also have been proposed. In ref. [41], the generalised symmetries, recursion operator and the integrability of eq. (2) with  $\alpha = -1$  have been studied. In ref. [42], a discrete coupled KdV-type equation hierarchy including eq. (2) as the first member has been derived from a  $4 \times 4$  matrix spectral problem, and the Hamiltonian structures and Liouville integrability also have been investigated for the obtained hierarchy. In ref. [43], the iterated DT for eq. (1) has been constructed from the standard Volterra equation based on its Lax pair in operator form, and some new explicit solutions in terms of Wronskians for eq. (1) have been given. However, to the best of our knowledge, the modulational instability (MI), discrete DT and generalised DT based on a  $4 \times 4$  Lax pair and some rational and semirational soliton solutions for eq. (1) have not been reported in the literature before.

Therefore, in this paper, we make further research on eq. (1) via the discrete DT and generalised DT based on the  $4 \times 4$  Lax pair. Unlike the previous studies, our DT in matrix form is different from the one in operator form in ref. [43]. Especially, we shall generalise our proposed usual DT to the generalised DT, then use it to derive some new rational and semirational soliton solutions for eq. (1), and the dynamical behaviours of such rational and semirational soliton solutions are numerically studied. The paper is organised as follows. In §2, the MI of constant seed background of eq. (1) will be analysed. In §3, the new DT in matrix form for eq. (1) will be constructed based on its new  $4 \times 4$  Lax pair, and then the generalised DT for eq. (1) will be proposed by using the Taylor expansion and a limit procedure. In §4, the soliton solution in terms of determinants will be explicitly derived via the usual discrete DT. In §5, the rational and semirational soliton solutions in terms of determinants will be explicitly given via the discrete generalised DT. In §6, the dynamical behaviour for such obtained soliton solutions will be analysed by means of numerical simulations. Some conclusions and discussions will be given in the final section.

## 2. MI of the non-zero seed state of eq. (1)

Equation (1) admits the following steady-state solution:

$$u_0 = a, \quad v_0 = b, \quad (5)$$

where  $a$  and  $b$  are real amplitudes. For the perturbation

$$u_n = a + \varepsilon p_n, \quad v_n = b + \varepsilon q_n, \quad (6)$$

where  $\varepsilon$  is an infinitely small amplitude of perturbation. Substituting eq. (6) into eq. (1) yields the real linearised system

$$\begin{aligned} p_{n,t} - a(p_{n+1} - p_{n-1}) + b(q_{n+1} - q_{n-1}) &= 0, \\ q_{n,t} - a(q_{n+1} - q_{n-1}) - b(p_{n+1} - p_{n-1}) &= 0. \end{aligned} \quad (7)$$

The solutions of eq. (7) are sought in the form

$$p_n = H e^{gt+ikn}, \quad q_n = K e^{gt+ikn}, \quad (8)$$

where  $i$  is the imaginary unit and  $i^2 = -1$ ,  $H$  and  $K$  are real constant amplitudes of the perturbation eigenmode,  $g$  denotes the MI gain and  $k$  is the arbitrary real wave number of a small perturbation. Substituting (8) into eq. (7), we have the following coupled equations:

$$\begin{aligned} 2iaH \sin(k) - 2ibK \sin(k) - Hg &= 0, \\ 2ibH \sin(k) + 2iaK \sin(k) - Kg &= 0. \end{aligned} \quad (9)$$

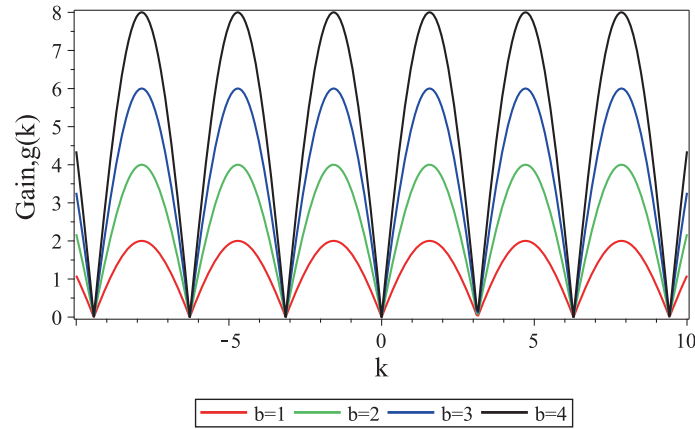


**Figure 1.** Gain spectra of the MI for the constant seed state amplitudes with the positive growth rate  $g(k)$ . Different lines correspond to values of the constant seed state amplitude  $b = 1$  (red line),  $b = 2$  (green line),  $b = 3$  (blue line) and  $b = 4$  (black line), as indicated in the figure.

We can easily obtain the following condition for the existence of non-trivial solutions  $H$  and  $K$  as

$$\begin{vmatrix} 2ia \sin(k) - g & -2ib \sin(k) \\ 2ib \sin(k) & 2ia \sin(k) - g \end{vmatrix} = 0 \quad (10)$$

$$E\varphi_n = \varphi_{n+1} = U_n\varphi_n = \begin{pmatrix} \lambda & -1 & 0 & 0 \\ \lambda u_n & 0 & \lambda v_n & 0 \\ 0 & 0 & \lambda & -1 \\ -\lambda v_n & 0 & \lambda u_n & 0 \end{pmatrix} \varphi_n, \quad (12)$$

$$\varphi_{n,t} = V_n\varphi_n = \begin{pmatrix} \frac{1}{2}\lambda + u_{n-1} & -1 & v_{n-1} & 0 \\ \lambda u_{n-1} & -\frac{1}{2}\lambda + u_n & \lambda v_{n-1} & v_n \\ -v_{n-1} & 0 & \frac{1}{2}\lambda + u_{n-1} & -1 \\ -v_{n-1}\lambda & -v_n & \lambda u_{n-1} & -\frac{1}{2}\lambda + u_n \end{pmatrix} \varphi_n, \quad (13)$$

or

$$g = \pm 2b \sin(k) + 2ia \sin(k). \quad (11)$$

If we assume that  $a = 0$  and  $b \neq 0$ ,  $g$  is real. Thus, the MI occurs if the right-hand side of (11) is positive, i.e. if  $b \neq 0$  and  $k \neq m\pi$ ,  $m \in \mathbb{Z}$ . Figure 1 shows the gain  $g(k)$  for  $b = 1, 2, 3$  and  $4$  at four power levels. Furthermore, at the point  $k = m\pi + \frac{1}{2}\pi$ ,  $m \in \mathbb{Z}$ , the function  $g^2$  attains its maximum  $g_{\max}^2 = 4b^2$ , so that the constant seed states are subject to MI and rational or semirational soliton solutions can be solutions of eq. (1).

### 3. The discrete DT and generalised DT

In [42], a hierarchy including eq. (2) has been derived from a  $4 \times 4$  matrix spectral problem. From this hierarchy, we can give the  $4 \times 4$  Lax pair of eq. (2). It is worth noting that we have changed the  $4 \times 4$  Lax pair in ref. [42] in order to better construct the DT and generalised DT of eq. (1) later. Equation (1) admits the following new Lax pair:

where  $E$  denotes the shift operator,  $\varphi_n = (\zeta_n, \phi_n, \psi_n, \omega_n)^T$  is the vector eigenfunction (T denotes the transpose),  $\lambda$  is the spectral parameter independent of  $n$  and  $t$ , and the shift operator  $E$  is defined by  $Ef_n = Ef(n, t) = f(n+1, t) \equiv f_{n+1}$ ,  $f_{n-1} = E^{-1}f(n, t) = f(n-1, t) \equiv f_{n-1}$ ,  $n \in \mathbb{Z}$ ,  $E \in \mathbb{R}$ . The zero curvature equation  $U_{n,t} + U_n V_n - V_{n+1} U_n = 0$  leads to eq. (1).

Let us consider a gauge transformation

$$\tilde{\varphi}_n = T_n \varphi_n, \quad (14)$$

where  $T_n$  is the Darboux matrix defined by

$$\tilde{U}_n = T_{n+1} U_n T_n^{-1}, \quad \tilde{V}_n = (T_{n,t} + T_n V_n) T_n^{-1}. \quad (15)$$

Lax pair (12) and (13) can be transformed into

$$\tilde{\varphi}_{n+1} = \tilde{U}_n \tilde{\varphi}_n, \quad \tilde{\varphi}_{n,t} = \tilde{V}_n \tilde{\varphi}_n, \quad (16)$$

where the matrices  $\tilde{U}_n$  and  $\tilde{V}_n$  have the same forms as  $U_n$  and  $V_n$  except that  $u_n$  and  $v_n$  are replaced by  $\tilde{u}_n$  and  $\tilde{v}_n$ . To guarantee the accuracy of the DT of eq. (1), we need to emphasise that the construction of the Darboux

matrix  $T_n$  is crucial. Here, a special Darboux matrix  $T_n$  is defined as

$$T_n = \begin{pmatrix} \lambda & a_n - 1 & 0 & b_n \\ c_n \lambda & a_n \lambda & d_n \lambda & b_n \lambda \\ 0 & -b_n & \lambda & a_n - 1 \\ -d_n \lambda & -b_n \lambda & c_n \lambda & a_n \lambda \end{pmatrix}, \tag{17}$$

where  $a_n, b_n, c_n, d_n$ , which are unknown functions of  $n$  and  $t$ , can be determined by solving the linear algebraic system  $T_n(\lambda_1)\varphi_n(\lambda_1) = 0$ , i.e.

$$\begin{aligned} \lambda_1 \zeta_n + (a_n - 1)\phi_n + b_n \omega_n &= 0, \\ c_n \zeta_n + a_n \phi_n + d_n \psi_n + b_n \omega_n &= 0, \\ -b_n \phi_n + \lambda_1 \psi_n + (a_n - 1)\omega_n &= 0, \\ -d_n \zeta_n - b_n \phi_n + c_n \psi_n + a_n \omega_n &= 0, \end{aligned} \tag{18}$$

where  $\varphi_n(\lambda_1) = (\zeta_n, \phi_n, \psi_n, \omega_n) = (\zeta_n(\lambda_1), \phi_n(\lambda_1), \psi_n(\lambda_1), \omega_n(\lambda_1))$  is one real solution of Lax pair (12) and (13). When  $\lambda_1$  is suitably chosen such that the determinant of coefficients for eq. (18) is non-zero, we can determine  $a_n, b_n, c_n, d_n$  uniquely. By applying these facts, we have the following theorem for the discrete DT of eq. (1).

**Theorem 1.** *Matrices  $\tilde{U}_n$  and  $\tilde{V}_n$  defined by eq. (15) have the same forms as  $U_n$  and  $V_n$ , where the DT formulae from the old potentials  $u_n$  and  $v_n$  into new potentials  $\tilde{u}_n$  and  $\tilde{v}_n$  are given by*

$$\begin{aligned} \tilde{u}_n &= \tilde{u}(n, t) = c_{n+1} + a_{n+1}u_n - b_{n+1}v_n, \\ \tilde{v}_n &= \tilde{v}(n, t) = d_{n+1} + b_{n+1}u_n + a_{n+1}v_n, \end{aligned} \tag{19}$$

where

$$a_n = \frac{\Delta a_n}{\Delta_1}, \quad b_n = \frac{\Delta b_n}{\Delta_1}, \quad c_n = \frac{\Delta c_n}{\Delta_2}, \quad d_n = \frac{\Delta d_n}{\Delta_2} \tag{20}$$

with

$$\begin{aligned} \Delta a_n &= \begin{vmatrix} \phi_n - \lambda_1 \zeta_n & \omega_n \\ \omega_n - \lambda_1 \psi_n & -\phi_n \end{vmatrix}, \\ \Delta b_n &= \begin{vmatrix} \phi_n & \phi_n - \lambda_1 \zeta_n \\ \omega_n & \omega_n - \lambda_1 \psi_n \end{vmatrix}, \\ \Delta_1 &= \begin{vmatrix} \phi_n & \omega_n \\ \omega_n & -\phi_n \end{vmatrix}, \\ \Delta c_n &= -a_n \begin{vmatrix} \phi_n & \psi_n \\ \omega_n & -\zeta_n \end{vmatrix} - b_n \begin{vmatrix} \omega_n & \psi_n \\ -\phi_n & -\zeta_n \end{vmatrix}, \\ \Delta d_n &= -a_n \begin{vmatrix} \zeta_n & \phi_n \\ \psi_n & \omega_n \end{vmatrix} - b_n \begin{vmatrix} \zeta_n & \omega_n \\ \psi_n & -\phi_n \end{vmatrix}, \\ \Delta_2 &= \begin{vmatrix} \zeta_n & \psi_n \\ \psi_n & -\zeta_n \end{vmatrix} \end{aligned}$$

and  $\Delta a_{n+1}, \Delta b_{n+1}, \Delta c_{n+1}$  and  $\Delta d_{n+1}$  can be gained from  $\Delta a_n, \Delta b_n, \Delta c_n$  and  $\Delta d_n$ , respectively, by substituting  $n$  with  $n + 1$ .

In fact, Theorem 1 proves the invariance form for  $U_n, V_n$  and  $\tilde{U}_n, \tilde{V}_n$  (the reader may refer to refs [23–36] and references therein). The proof is similar and not presented here. By using Theorem 1, the soliton solutions of eq. (1) can be derived with the initial constant seed solutions  $u_n = a$  and  $v_n = b$  in the next section. However, this is not the main aim of this paper. Our aim is to extend the usual DT to generate the generalised DT such that the rational and semirational soliton solutions in terms of determinants of eq. (1) can be given. Next, we shall construct the generalised DT of eq. (1) based on DT in the matrix form. The main difference between DT and the generalised DT is that the former can give the soliton solution, whereas the latter can derive the rational and semirational soliton solutions. To derive the rational and semirational soliton solutions, we need to consider the Taylor expansion of  $T_n \varphi_n|_{\lambda=\lambda_1+\varepsilon} = T_n(\lambda_1 + \varepsilon)\varphi_n(\lambda_1 + \varepsilon)$  at  $\varepsilon = 0$ . We know that

$$T_n(\lambda_1 + \varepsilon) = T_n^{(1)}\varepsilon + T_n^{(0)} \tag{21}$$

and

$$\varphi_n(\varepsilon) = \varphi_n^{(0)} + \varphi_n^{(1)}\varepsilon + \varphi_n^{(2)}\varepsilon^2 + \varphi_n^{(3)}\varepsilon^3 + \dots, \tag{22}$$

where

$$\begin{aligned} \varphi_n^{(k)}(\lambda_1) &= \left( \zeta_n^{(k)}, \phi_n^{(k)}, \psi_n^{(k)}, \omega_n^{(k)} \right)^T \\ &= \left( \frac{1}{k!} \frac{\partial^k}{\partial \lambda_1^k} \zeta_n, \frac{1}{k!} \frac{\partial^k}{\partial \lambda_1^k} \phi_n, \frac{1}{k!} \frac{\partial^k}{\partial \lambda_1^k} \psi_n, \frac{1}{k!} \frac{\partial^k}{\partial \lambda_1^k} \omega_n \right)^T \end{aligned}$$

with  $\varphi_n^{(0)} = (\zeta_n^{(0)}, \phi_n^{(0)}, \psi_n^{(0)}, \omega_n^{(0)})^T$  ( $k = 0, 1, 2, 3, \dots$ ).

Therefore, when  $\varepsilon \rightarrow 0$ , we can obtain the new linear algebraic system  $T_n^{(0)}\varphi_n^{(0)} = 0$  which is similar to system (18), from which we can derive new  $a_n, b_n, c_n, d_n$ . So we can give the discrete generalised DT of eq. (1) described by the following theorem.

**Theorem 2.** *Let  $\varphi_n(\lambda_1) = (\zeta_n, \phi_n, \psi_n, \omega_n)^T$  be the one column-vector solution of Lax pair (12) and (13) for spectral parameters  $\lambda_1$  and the non-zero initial solutions  $u_n$  and  $v_n$  of eq. (1). Then the generalised DT of eq. (1) is obtained by*

$$\begin{aligned} \tilde{u}_n &= \tilde{u}(n, t) = c_{n+1} + a_{n+1}u_n - b_{n+1}v_n, \\ \tilde{v}_n &= \tilde{v}(n, t) = d_{n+1} + b_{n+1}u_n + a_{n+1}v_n \end{aligned} \tag{23}$$

with

$$a_n = \frac{\Delta a_n}{\Delta_1}, \quad b_n = \frac{\Delta b_n}{\Delta_1},$$

$$c_n = \frac{\Delta c_n}{\Delta_2}, \quad d_n = \frac{\Delta d_n}{\Delta_2}, \tag{24}$$

where

$$\begin{aligned} \Delta a_n &= \begin{vmatrix} \phi_n^{(0)} - \lambda_1 \zeta_n^{(0)} & \omega_n^{(0)} \\ \omega_n^{(0)} - \lambda_1 \psi_n^{(0)} & -\phi_n^{(0)} \end{vmatrix}, \\ \Delta b_n &= \begin{vmatrix} \phi_n^{(0)} & \phi_n^{(0)} - \lambda_1 \zeta_n^{(0)} \\ \omega_n^{(0)} & \omega_n^{(0)} - \lambda_1 \psi_n^{(0)} \end{vmatrix}, \\ \Delta_1 &= \begin{vmatrix} \phi_n^{(0)} & \omega_n^{(0)} \\ \omega_n^{(0)} & -\phi_n^{(0)} \end{vmatrix}, \\ \Delta c_n &= -a_n \begin{vmatrix} \phi_n^{(0)} & \psi_n^{(0)} \\ \omega_n^{(0)} & -\zeta_n^{(0)} \end{vmatrix} - b_n \begin{vmatrix} \omega_n^{(0)} & \psi_n^{(0)} \\ -\phi_n^{(0)} & -\zeta_n^{(0)} \end{vmatrix}, \\ \Delta d_n &= -a_n \begin{vmatrix} \zeta_n^{(0)} & \phi_n^{(0)} \\ \psi_n^{(0)} & \omega_n^{(0)} \end{vmatrix} - b_n \begin{vmatrix} \zeta_n^{(0)} & \omega_n^{(0)} \\ \psi_n^{(0)} & -\phi_n^{(0)} \end{vmatrix}, \\ \Delta_2 &= \begin{vmatrix} \zeta_n^{(0)} & \psi_n^{(0)} \\ \psi_n^{(0)} & -\zeta_n^{(0)} \end{vmatrix}, \end{aligned}$$

where  $\zeta_n^{(0)}, \phi_n^{(0)}, \psi_n^{(0)}$  and  $\omega_n^{(0)}$  are obtained from (22), and  $\Delta a_{n+1}, \Delta b_{n+1}, \Delta c_{n+1}$  and  $\Delta d_{n+1}$  can be gained from  $\Delta a_n, \Delta b_n, \Delta c_n$  and  $\Delta d_n$ , respectively, by substituting  $n + 1$  for  $n$ .

#### 4. Soliton solutions of eq. (1) from non-vanishing background

By using DT in Theorem 1, we can give the soliton solutions of eq. (1). Substituting the initial solutions  $u_n = c$  and  $v_n = 0$  into (12) and (13) can give one basic solution of Lax pair (12) and (13) with the spectral parameter  $\lambda = \lambda_1$  as follows:

$$\begin{aligned} \varphi(\lambda_1) &= \begin{pmatrix} \zeta_n \\ \phi_n \\ \psi_n \\ \omega_n \end{pmatrix} = \tau_1^{n-1} e^{\rho_1 t} \begin{bmatrix} C_1 \tau_1 \\ c C_1 \lambda_1 \\ C_3 \tau_1 \\ c C_3 \lambda_1 \end{bmatrix} \\ &+ \tau_2^{n-1} e^{\rho_2 t} \begin{bmatrix} C_2 \tau_2 \\ c C_2 \lambda_1 \\ C_4 \tau_2 \\ c C_4 \lambda_1 \end{bmatrix} \end{aligned} \tag{25}$$

with

$$\begin{aligned} \tau_1 &= \frac{1}{2} \lambda_1 + \frac{1}{2} \sqrt{\lambda_1^2 - 4c\lambda_1}, \quad \tau_2 = \frac{1}{2} \lambda_1 - \frac{1}{2} \sqrt{\lambda_1^2 - 4c\lambda_1}, \\ \rho_1 &= c + \frac{1}{2} \sqrt{\lambda_1^2 - 4c\lambda_1}, \quad \rho_2 = c - \frac{1}{2} \sqrt{\lambda_1^2 - 4c\lambda_1}, \end{aligned}$$

where  $C_1, C_2, C_3$  and  $C_4$  are arbitrary real constants. Solving system (18) leads to

$$a_n = \frac{\Delta a_n}{\Delta_1}, \quad b_n = \frac{\Delta b_n}{\Delta_1}, \quad c_n = \frac{\Delta c_n}{\Delta_2}, \quad d_n = \frac{\Delta d_n}{\Delta_2}, \tag{26}$$

where

$$\begin{aligned} \Delta a_n &= \begin{vmatrix} \phi_n - \lambda_1 \zeta_n & \omega_n \\ \omega_n - \lambda_1 \psi_n & -\phi_n \end{vmatrix}, \\ \Delta b_n &= \begin{vmatrix} \phi_n & \phi_n - \lambda_1 \zeta_n \\ \omega_n & \omega_n - \lambda_1 \psi_n \end{vmatrix}, \quad \Delta_1 = \begin{vmatrix} \phi_n & \omega_n \\ \omega_n & -\phi_n \end{vmatrix}, \\ \Delta c_n &= -a_n \begin{vmatrix} \phi_n & \psi_n \\ \omega_n & -\zeta_n \end{vmatrix} - b_n \begin{vmatrix} \omega_n & \psi_n \\ -\phi_n & -\zeta_n \end{vmatrix}, \\ \Delta d_n &= -a_n \begin{vmatrix} \zeta_n & \phi_n \\ \psi_n & \omega_n \end{vmatrix} - b_n \begin{vmatrix} \zeta_n & \omega_n \\ \psi_n & -\phi_n \end{vmatrix}, \\ \Delta_2 &= \begin{vmatrix} \zeta_n & \psi_n \\ \psi_n & -\zeta_n \end{vmatrix}, \end{aligned}$$

where  $a_{n+1}, b_{n+1}, c_{n+1}$  and  $d_{n+1}$  can be derived from  $a_n, b_n, c_n$  and  $d_n$ , respectively by replacing  $n$  with  $n + 1$ . By applying (19), we can give the soliton solutions as follows:

$$\begin{aligned} \tilde{u}_n &= \tilde{u}(n, t) = c_{n+1} + a_{n+1}c, \\ \tilde{v}_n &= \tilde{v}(n, t) = d_{n+1} + b_{n+1}c. \end{aligned} \tag{27}$$

With symbolic computation and choosing the special parameters  $c = \frac{1}{4}, \lambda = C_1 = 4, C_2 = 3, C_3 = 2, C_4 = 1$ , the expression for (27) can be simplified to provide the solution

$$\tilde{u}_n = \frac{\Omega_1}{\Omega_2}, \quad \tilde{v}_n = \frac{\Omega_3}{\Omega_4} \tag{28}$$

with

$$\begin{aligned} \Omega_1 &= (\sqrt{3} - 2) [100\sqrt{3}(97 + 56\sqrt{3})^n e^{8\sqrt{3}t} \\ &- 7840\sqrt{3}(7 - 4\sqrt{3})^n e^{2\sqrt{3}t} \\ &- 375\sqrt{3}(97 - 56\sqrt{3})^n - 10496\sqrt{3}e^{4\sqrt{3}t} \\ &+ 3920(7 + 4\sqrt{3})^n \\ &+ 200(97 + 56\sqrt{3})^n e^{8\sqrt{3}t} + 13720(7 - 4\sqrt{3})^n e^{2\sqrt{3}t} \\ &+ 650(97 - 56\sqrt{3})^n + 20992e^{4\sqrt{3}t}], \end{aligned}$$

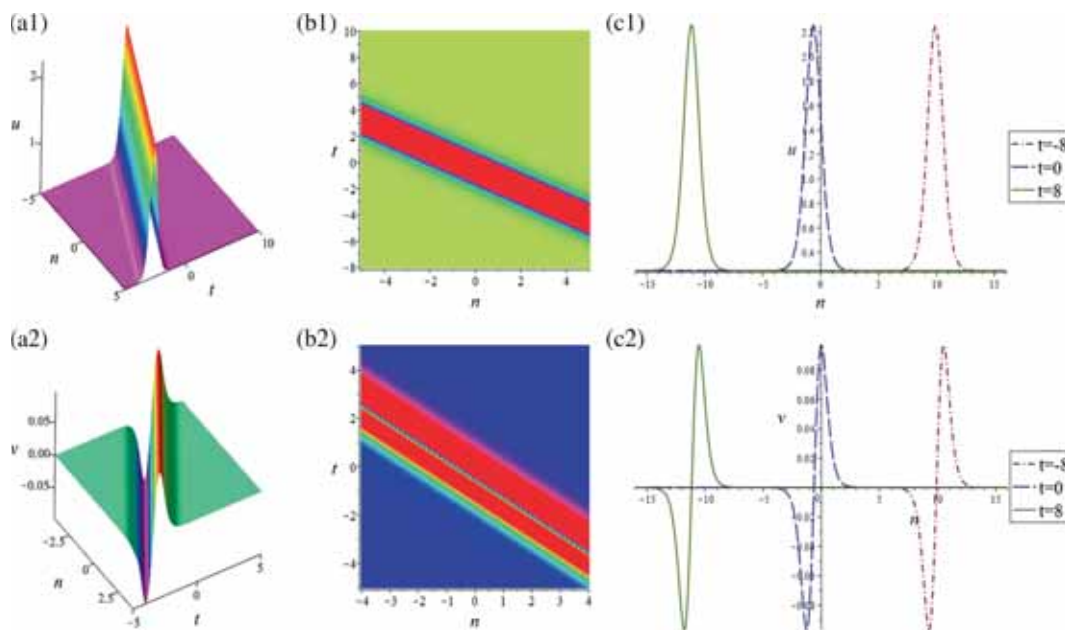


**Figure 2.** One-soliton solution (27) with the parameters  $c = \frac{1}{4}, \lambda = C_1 = 4, C_2 = 3, C_3 = 2, C_4 = 1$ . (a1) and (b1) show the component  $u_n$ , (a2) and (b2) show the component  $v_n$ , (c1) shows the propagation processes for  $u_n$  and (c2) shows the propagation processes for  $v_n$  at  $t = -8$  (dash-dotted line),  $t = 0$  (long-dashed line) and  $t = 8$  (solid line).

$$\begin{aligned} \Omega_2 &= 4[280\sqrt{3}(7-4\sqrt{3})^n + 56\sqrt{3}e^{2\sqrt{3}t} \\ &\quad - 10(7 + 4\sqrt{3})^n e^{4\sqrt{3}t} \\ &\quad - 485(7 - 4\sqrt{3})^n - 98e^{2\sqrt{3}t}] \\ &\quad \times [10(7+4\sqrt{3})^n e^{4\sqrt{3}t} + 14e^{2\sqrt{3}t} + 5(7 - 4\sqrt{3})^n], \\ \Omega_3 &= 60(\sqrt{3} - 2)e^{(1/2)t} [4\sqrt{3}(7-4\sqrt{3})^n e^{(1/2)(4\sqrt{3}-1)t} \\ &\quad + 2(7 + 4\sqrt{3})^n e^{(1/2)(12\sqrt{3}-1)t} \\ &\quad - 7(7 - 4\sqrt{3})^n e^{(1/2)(4\sqrt{3}-1)t}], \\ \Omega_4 &= [280\sqrt{3}(7 - 4\sqrt{3})^n + 56\sqrt{3}e^{2\sqrt{3}t} \\ &\quad - 10(7 + 4\sqrt{3})^n e^{4\sqrt{3}t} \\ &\quad - 485(7 - 4\sqrt{3})^n - 98e^{2\sqrt{3}t}] \\ &\quad \times [10(7+4\sqrt{3})^n e^{4\sqrt{3}t} + 14e^{2\sqrt{3}t} + 5(7 - 4\sqrt{3})^n]. \end{aligned}$$

Figure 2 shows one-soliton structures of  $\tilde{u}_n$  and  $\tilde{v}_n$  in solution (27). From figure 2, we can see that solution  $u_n$  has a bell-shaped one-soliton structure, whereas  $v_n$  has a staggered anti- $N$ -shaped one-soliton structure. Both one-solitons  $\tilde{u}_n$  and  $\tilde{v}_n$  propagate along the negative  $n$ -axis with the increasing time. The maximum amplitude of  $u_n$  is about 2.2567 and almost along the line  $n + 1.315t + 0.632 = 0$ , while for solution  $v_n$ , the maximum and minimum amplitudes are about 0.0969 and  $-0.0969$  and almost along two lines  $n + 1.315t + 1.262 = 0$  and  $n + 1.315t + 0.001 = 0$ , respectively. The evolution velocities of  $\tilde{u}_n$  and  $\tilde{v}_n$  are about 1.315.

### 5. Rational and semirational soliton solutions of eq. (1)

In this section, we shall use the generalised DT in Theorem 2 to derive some rational and semirational soliton solutions of eq. (1).

#### 5.1 Rational soliton solutions of eq. (1)

In what follows, the spectral parameter  $\lambda = \lambda_1 + \varepsilon^2$  with  $\lambda_1 = 4c$  in eq. (25) is fixed. Then the vector function  $\varphi$  in eq. (25) is expanded as four Taylor series around  $\varepsilon = 0$ . To derive the rational soliton solutions of eq. (1), here we choose some special parameters  $c, \lambda, C_1, C_2, C_3, C_4$  (e.g.  $c = \frac{1}{4}, \lambda_1 = C_1 = -C_2 = 1, C_3 = C_4 = \varepsilon$ ) and then obtain

$$\varphi(\varepsilon^2) = \varphi^{(0)} + \varphi^{(1)}\varepsilon^2 + \varphi^{(2)}\varepsilon^4 + \varphi^{(3)}\varepsilon^6 + \dots, \quad (29)$$

where

$$\varphi^{(0)} = \begin{pmatrix} \xi^{(0)} \\ \phi^{(0)} \\ \psi^{(0)} \\ \omega^{(0)} \end{pmatrix} = \frac{1}{2^n} e^{(1/4)t} \begin{pmatrix} 2n + t \\ n + \frac{1}{2}t - 1 \\ 2 \\ 1 \end{pmatrix}.$$

In Theorem 2,  $\varphi^{(0)}$  is only used in the generalised DT. So we only list  $\varphi^{(0)}$  and the rest  $\varphi^{(i)} (i \geq 1)$  are omitted here. Using (23) and (24), we can give the rational soliton solutions as follows:

$$\begin{aligned} \tilde{u}_n &= \tilde{u}(n, t) = c_{n+1} + a_{n+1}c, \\ \tilde{v}_n &= \tilde{v}(n, t) = d_{n+1} + b_{n+1}c. \end{aligned} \tag{30}$$

With the aid of symbolic computation, the simplification form of solution (30) is obtained as follows:

$$\tilde{u}_n = \frac{[(2n + t + 1)^2 - 1]^2 + 64}{4[(2n + t + 1)^2 + 3]^2 + 64},$$

soliton solutions, and we here call them the so-called semirational soliton solutions. Next, we fix  $\lambda = \lambda_1 + \varepsilon^2$  with  $\lambda_1 = 4c + 1$ . The vector function  $\varphi$  in eq. (25) is extended as four Taylor series around  $\varepsilon = 0$ . Here we choose some special parameters  $c, \lambda, C_1, C_2, C_3, C_4$  (e.g.  $c = \frac{1}{4}, \lambda_1 = 2, C_1 = -C_2 = C_3 = C_4 = \varepsilon$ ) and then have

$$\varphi(\varepsilon^2) = \varphi^{(0)} + \varphi^{(1)}\varepsilon^2 + \varphi^{(2)}\varepsilon^4 + \varphi^{(3)}\varepsilon^6 + \dots, \tag{32}$$

where

$$\varphi^{(0)} = \begin{pmatrix} \zeta^{(0)} \\ \phi^{(0)} \\ \psi^{(0)} \\ \omega^{(0)} \end{pmatrix} = \begin{pmatrix} \frac{-8(1+\frac{1}{2}\sqrt{2})^n e^{(1/4)(1+2\sqrt{2})t} + 8(1-\frac{1}{2}\sqrt{2})^n e^{(1/4)(1-2\sqrt{2})t}}{(2+\sqrt{2})^3(\sqrt{2}-2)^3} \\ \frac{4(2+\sqrt{2})(1-\frac{1}{2}\sqrt{2})^n e^{(1/4)(1-2\sqrt{2})t} + 4(\sqrt{2}-2)(1+\frac{1}{2}\sqrt{2})^n e^{(1/4)(1+2\sqrt{2})t}}{(2+\sqrt{2})^3(\sqrt{2}-2)^3} \\ \frac{-8(1+\frac{1}{2}\sqrt{2})^n e^{(1/4)(1+2\sqrt{2})t} - 8(1-\frac{1}{2}\sqrt{2})^n e^{(1/4)(1-2\sqrt{2})t}}{(2+\sqrt{2})^3(\sqrt{2}-2)^3} \\ \frac{-4(2+\sqrt{2})(1-\frac{1}{2}\sqrt{2})^n e^{(1/4)(1-2\sqrt{2})t} + 4(\sqrt{2}-2)(1+\frac{1}{2}\sqrt{2})^n e^{(1/4)(1+2\sqrt{2})t}}{(2+\sqrt{2})^3(\sqrt{2}-2)^3} \end{pmatrix}.$$

$$\tilde{v}_n = \frac{-8(2n + t + 1)}{[(2n + t + 1)^2 + 3]^2 + 16}, \tag{31}$$

which have no singular points for all real  $n$  and  $t$ . Figure 3 displays the first-order  $W$ -shaped soliton structure of solution  $\tilde{u}_n$  in (31) and a staggered first-order  $N$ -shaped soliton structure of solution  $\tilde{v}_n$  in (31). Both first-order rational solitons  $\tilde{u}_n$  and  $\tilde{v}_n$  propagate along the negative  $n$ -axis with increasing time. The evolution velocities of both  $\tilde{u}_n$  and  $\tilde{v}_n$  are about 0.5. Soliton  $\tilde{u}_n$  given by solution (31) has properties:  $\min \tilde{u}_n = \frac{3}{4} - \frac{1}{4}\sqrt{5}$  as  $n = -\frac{1}{2}t - \frac{1}{2} \pm \frac{1}{2}\sqrt{5 + 4\sqrt{5}}$ ;  $\max \tilde{u}_n = \frac{13}{20}$  as  $n = -\frac{1}{2}t - \frac{1}{2}$ . Soliton  $\tilde{v}_n$  given by solution (31) has properties:  $\max \tilde{v}_n = -\frac{\sqrt{21}-11}{100}\sqrt{6\sqrt{21}-9}$  as  $n = -\frac{1}{2}t - \frac{1}{2} - \frac{1}{6}\sqrt{6\sqrt{21}-9}$ ;  $\min \tilde{v}_n = \frac{\sqrt{21}-11}{100}\sqrt{6\sqrt{21}-9}$  as  $n = -\frac{1}{2}t - \frac{1}{2} + \frac{1}{6}\sqrt{6\sqrt{21}-9}$ .

### 5.2 Semirational soliton solutions of eq. (1)

In the above subsection, we choose the spectral parameter  $\lambda_1 = 4c$  and give the rational soliton solutions of eq. (1), in which the numerator and denominator in solution (31) are the polynomials of  $n$  and  $t$ . In the following, we shall give some new soliton solutions, which are the combinations of exponential function and polynomial functions of  $n$  and  $t$  in the numerator and denominator, to distinguish the above rational

Here we only list  $\varphi^{(0)}$  and the rest  $\varphi^{(i)}$  ( $i \geq 1$ ) are omitted. By applying (23) and (24), we can give the semirational soliton solutions as follows:

$$\begin{aligned} \tilde{u}_n &= \tilde{u}(n, t) = c_{n+1} + a_{n+1}c, \\ \tilde{v}_n &= \tilde{v}(n, t) = d_{n+1} + b_{n+1}c, \end{aligned} \tag{33}$$

where  $a_{n+1}, b_{n+1}, c_{n+1}$  and  $d_{n+1}$  are the same as those in the above subsection. With symbolic computation, the simplification forms of semirational soliton solution (33) are given as

$$\tilde{u}_n = \tilde{u}(n, t) = \frac{\Gamma_1}{\Gamma_2}, \quad \tilde{v}_n = \tilde{v}(n, t) = \frac{\Gamma_3}{\Gamma_4} \tag{34}$$

with

$$\begin{aligned} \Gamma_1 &= -8^{-n}(2\sqrt{2} + 41)[(12576 - 8448\sqrt{2}) \\ &\quad \times (3 + 2\sqrt{2})^{-n} e^{2\sqrt{2}t} \\ &\quad + (8284\sqrt{2} - 10887)(3 - 2\sqrt{2})^n e^{2\sqrt{2}t} \\ &\quad + (131 - 88\sqrt{2})(99 - 70\sqrt{2})^n \\ &\quad + (115 + 76\sqrt{2})(99 + 70\sqrt{2})^n e^{6\sqrt{2}t} \\ &\quad + 1673(3 + 2\sqrt{2})^n e^{4\sqrt{2}t}], \\ \Gamma_2 &= 8^{-n}(8\sqrt{2} - 12)[(12\sqrt{2} + 17)(99 + 70\sqrt{2})^n e^{6\sqrt{2}t} \\ &\quad + (12\sqrt{2} + 19)(3 - 2\sqrt{2})^n e^{2\sqrt{2}t} \\ &\quad + (24\sqrt{2} + 35)(3 + 2\sqrt{2})^n e^{4\sqrt{2}t} + (99 - 70\sqrt{2})^n], \end{aligned}$$

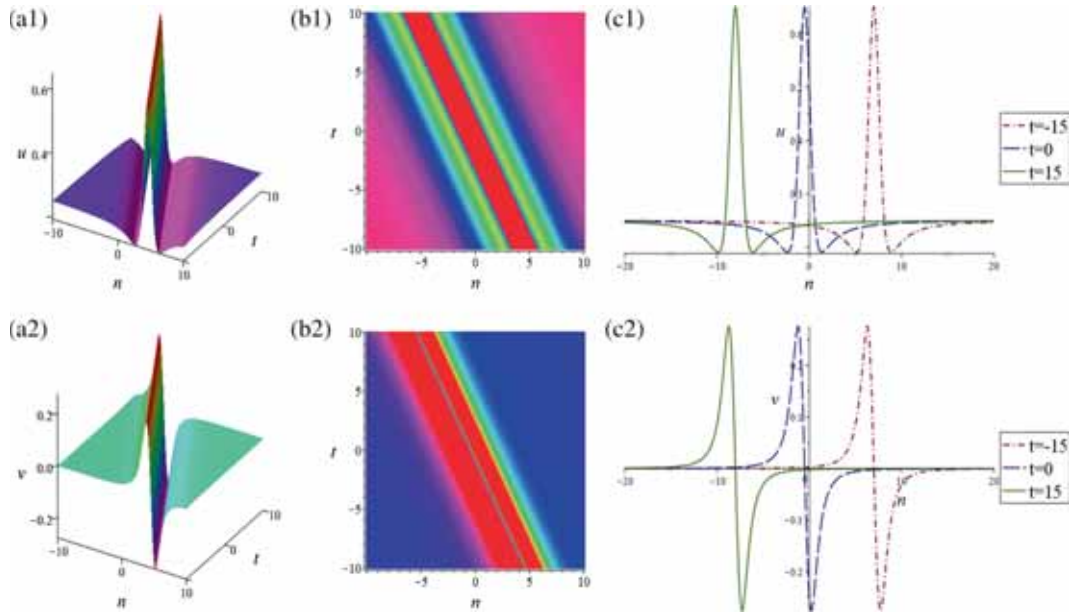


**Figure 3.** Rational soliton solution (30) with the parameters  $c = \frac{1}{4}, \lambda = 1, C_1 = -C_2 = 1, C_3 = C_4 = \varepsilon$ . (a1) and (b1) show the component  $u_n$ , (a2) and (b2) show the component  $v_n$ , (c1) shows the propagation processes for  $u_n$  and (c2) shows the propagation processes for  $v_n$  at  $t = -15$  (dash-dotted line),  $t = 0$  (long-dashed line) and  $t = 15$  (solid line).

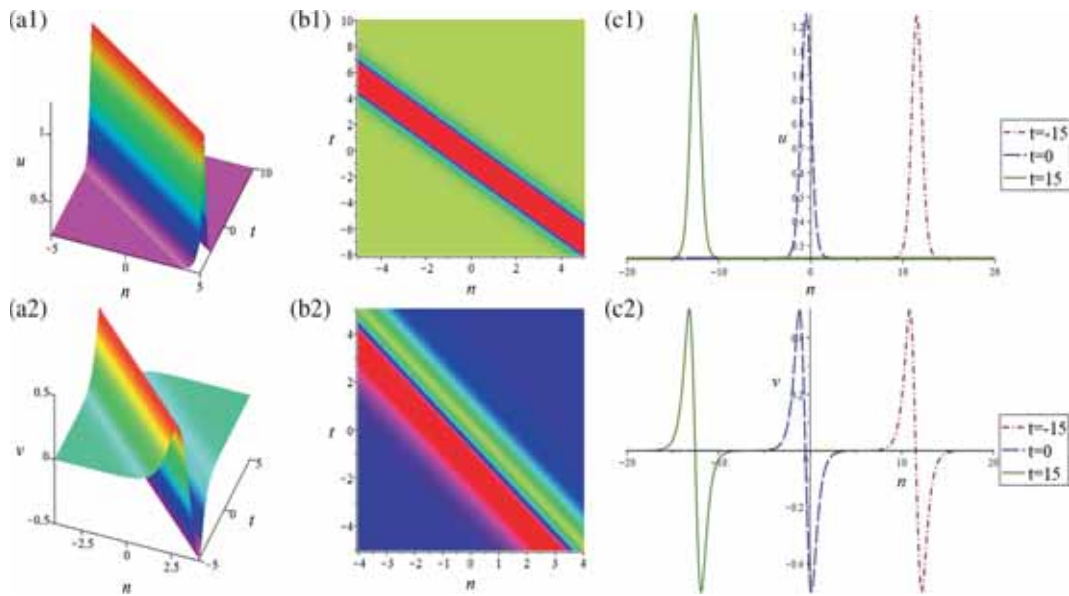
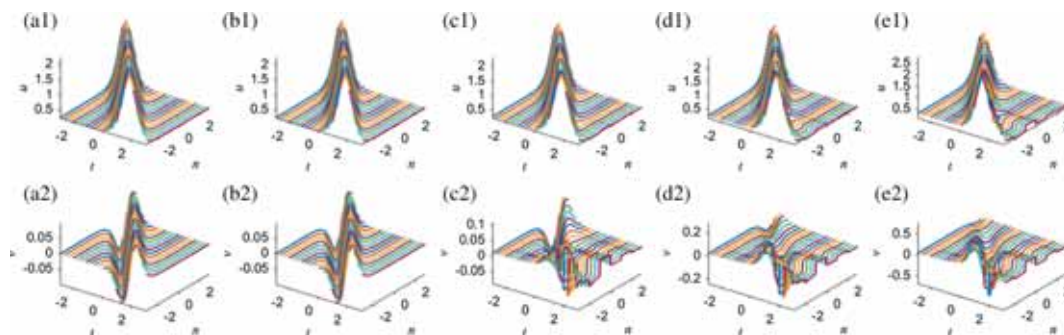


**Figure 4.** Semirational soliton solution (33) with the parameters  $c = \frac{1}{4}, \lambda = 2, C_1 = -C_2 = C_3 = C_4 = \varepsilon$ . (a1) and (b1) show the component  $u_n$ , (a2) and (b2) show the component  $v_n$ , (c1) shows the propagation processes for  $u_n$  and (c2) shows the propagation processes for  $v_n$  at  $t = -15$  (dash-dotted line),  $t = 0$  (long-dashed line) and  $t = 15$  (solid line).

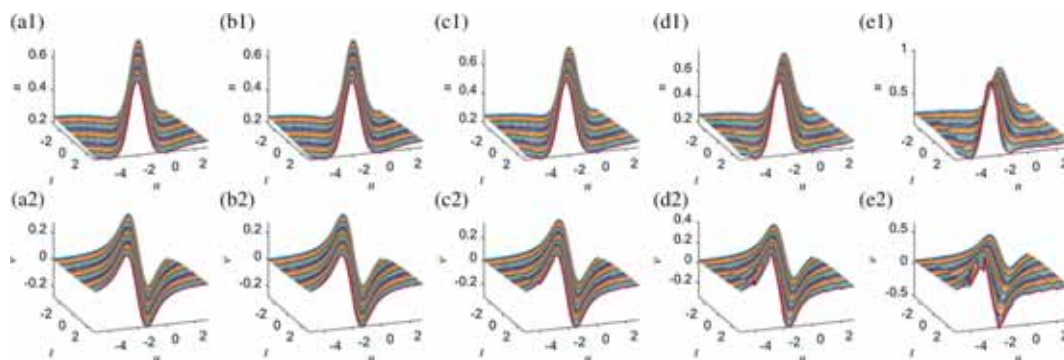
$$\begin{aligned} \Gamma_3 = & 16^{-n} \sqrt{2} e^{\sqrt{2}t} \left[ -2(2\sqrt{2} + 3)^{-n} e^{2\sqrt{2}t} \right. \\ & + 5(2\sqrt{2} + 3)^{-n} (17 + 12\sqrt{2})^n e^{4\sqrt{2}t} \\ & + (2\sqrt{2} + 3)^{n+1} e^{4\sqrt{2}t} - (2\sqrt{2} - 8) \\ & \times (3 - 2\sqrt{2})^n e^{2\sqrt{2}t} + (2 - 2\sqrt{2})(99 - 70\sqrt{2})^n \\ & \left. + (2 + 2\sqrt{2})(99 + 70\sqrt{2})^n e^{6\sqrt{2}t} \right], \end{aligned}$$

$$\begin{aligned} \Gamma_4 = & 16^{-n} (2\sqrt{2} - 3) \left[ (577 - 408\sqrt{2})^n \right. \\ & + (12\sqrt{2} + 20)(17 - 12\sqrt{2})^n e^{2\sqrt{2}t} \\ & + (36\sqrt{2} + 52)(17 + 12\sqrt{2})^n e^{6\sqrt{2}t} \\ & + (54 + 36\sqrt{2}) e^{4\sqrt{2}t} \\ & \left. + (12\sqrt{2} + 17)(577 + 408\sqrt{2})^n e^{8\sqrt{2}t} \right]. \end{aligned}$$





**Figure 5.** Numerical simulations for the soliton solution (27) with the same parameters as in figure 2. (a1) and (a2) show exact solution (27), (b1) and (b2) show numerical solution without noise, (c1) and (c2) show numerical solution with a 1% noise, (d1) and (d2) show numerical solution with a 2% noise and (e1) and (e2) show numerical solution with a 5% noise.



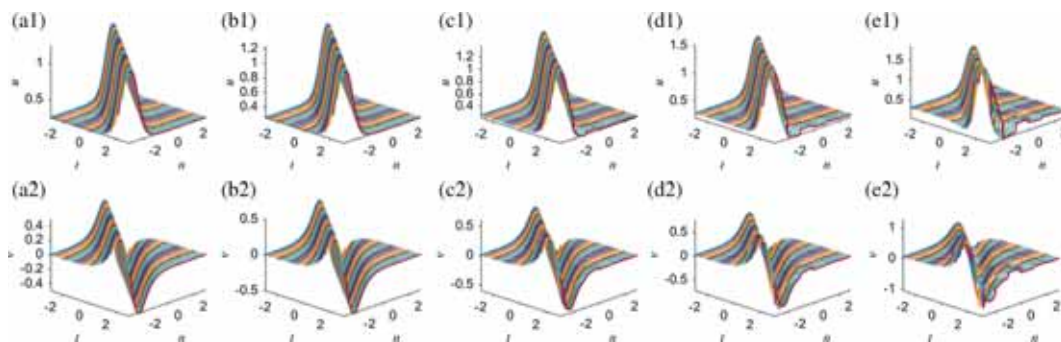
**Figure 6.** Numerical simulations for the rational soliton solution (30) with the same parameters as in figure 3. (a1) and (a2) show exact solution (30), (b1) and (b2) show numerical solution without noise, (c1) and (c2) show numerical solution with a 1% noise, (d1) and (d2) show numerical solution with a 2% noise and (e1) and (e2) show numerical solution with a 5% noise.

Figure 4 shows the first-order bell-shaped semirational soliton structure of solution  $\tilde{u}_n$  in (34) and the first-order staggered  $N$ -shaped semirational soliton structure of solution  $\tilde{v}_n$  in (34), from which we can see that they are similar to the one-soliton solution (28) in the previous section. Both first-order semisolitons  $\tilde{u}_n$  and  $\tilde{v}_n$  propagate along the negative  $n$ -axis with increasing time. The maximum amplitude of  $\tilde{u}_n$  is about 1.250 and almost along the line  $n + 0.802t + 0.150 = 0$ , while for solution  $\tilde{v}_n$ , the evolution velocity is about 0.0969, and the maximum and minimum amplitudes are about 0.5 and  $-0.5$  and almost along two lines  $n + 0.802t + 0.1502 = 0$  and  $n + 0.802t + 0.1504 = 0$ , respectively. Their evolution velocities are about 0.802.

*Remark 1.* Here we point out that we have substituted solutions (27), (30) and (33) into eq. (1) with the aid of the symbolic computation Maple, and they satisfy eq. (1) whose validity is verified by the symbolic computation Maple. In fact, the correctness of these solutions can also be verified by numerical simulation in the next section from which we can see that the numerical results almost agree with their corresponding exact solutions.

## 6. Dynamical behaviours of soliton solutions

Numerical simulation plays an important role in the investigation of nonlinear waves. To further study the wave propagations of some of the above-obtained soliton solutions, we shall study the dynamical behaviours of the soliton solution (27), the rational soliton solution (30) and the semirational soliton solution (33) by applying finite-difference method [44,45]. Figures 5–7 show the exact solutions (27), (30) and (33) of eq. (1), time evolutions of using the exact solutions (27), (30) and (33) and those perturbed by a small noise. Figures 5a1, 5b1, 5a2, 5b2 to 7a1, 7b1, 7a2, 7b2 show that the profiles of the time evolution of solutions (27), (30) and (33) without the addition of noise almost agree with the ones of the corresponding exact solutions (27), (30) and (33) in time  $t \in (-3, 3)$ , and it is clearly shown that solutions obtained by us and numerical scheme are accurate. Figures 5c1, 5c2, 5d1, 5d2 and 5e1, 5e2 to 7c1, 7c2, 7d1, 7d2 and 7e1, 7e2 display the numerical results of perturbed solutions (27), (30) and (33) by multiplying the exact solutions at  $t = -3$  by  $1 + 0.01\text{Random}[-3, 3]$ ,  $1 + 0.02\text{Random}[-3, 3]$  and  $1 + 0.05\text{Random}[-3, 3]$ ,



**Figure 7.** Numerical simulations for the semirational soliton solution (33) with the same parameters as in figure 4. (a1) and (a2) show exact solution (33), (b1) and (b2) show numerical solution without noise, (c1) and (c2) show numerical solution with a 1% noise, (d1) and (d2) show numerical solution without a 2% noise and (e1) and (e2) show numerical solution with a 5% noise.

respectively. For the soliton solution (27), the numerical results show that the 1% and 2% noises (see figures 5c1, 5d1 and 5e1) have almost no effect on the evolutions of  $u_n$  in (27) by comparing figures 5a1 and 5b1, while the 5% noise only has a slight effect on the evolution of  $u_n$ . However, these noises have an evident effect on the evolution of  $v_n$  in (27) by comparing figures 5a2 and 5b2. Especially with the noise increasing, the amplitudes of  $v_n$  appear to have bigger oscillation. For the soliton solution (30), the numerical results show that the 1%, 2% and 5% noises (see figures 6c1, 6d1 and 6e1) have almost no effect on the evolution of  $u_n$  and  $v_n$  in (30) by comparing figures 6a1, 6b1 and 6a2, 6b2. For the soliton solution (33), the numerical results show that the 1%, 2% and 5% noises (see figures 7c1, 7d1 and 7e1) have almost no effect on the evolution of  $u_n$  and  $v_n$  in (33) by comparing figures 7a1 and 7b1 except for smaller oscillation with a 5% noise. In summary, solutions (27), (30) and (33) are robust against a small noise, but the rational and semirational soliton solutions (30) and (33) have better numerical stability than the usual soliton solution (27).

## 7. Conclusions

In this paper, our main attention has been focussed on eq. (1) associated with the  $4 \times 4$  Lax pair. We have analytically constructed the discrete DT and generalised DT for eq. (1). Via the obtained DT, we have derived the discrete one-soliton solution (27) of eq. (1). Through the generalised DT, we have obtained the discrete rational and semirational soliton solutions (30) and (33) of eq. (1). Figure 2 shows a bell-shaped one-soliton structure of  $u_n$  and a staggered anti- $N$ -shaped one-soliton structure of  $v_n$  in (27). Figures 3 and 4 display the  $M$ -shaped and  $N$ -shaped rational soliton and bell-shaped and  $N$ -shaped semirational soliton solutions of

eq. (1). The numerical simulation results in figures 5–7 show that such soliton solutions have stable evolutions without noise and are robust against small noise. The results may be helpful for understanding some physical phenomena in fluids, Bose–Einstein condensation and atmospheric dynamics described by the coupled KdV equation. In addition, it should be pointed out that although we have constructed the first-order rational soliton and semirational soliton solutions of eq. (1), further research is needed about how to construct the higher-order rational soliton and semirational soliton solutions of eq. (1). We shall carry out further investigation in our future work.

## Acknowledgements

This work was partially supported by Qin Xin Talents Cultivation Program of Beijing Information Science and Technology University (QXTCP B201704), the NSFC under Grant Nos 11375030 and 61471406, the Beijing Natural Science Foundation under Grant No. 1153004.

## References

- [1] A M Wazwaz, *Pramana – J. Phys.* **87**: 68 (2016)
- [2] Y K Liu and B Li, *Pramana – J. Phys.* **88**: 57 (2017)
- [3] Z Du, B Tian, X Y Xie, J Chai and X Y Wu, *Pramana – J. Phys.* **90**: 45 (2018)
- [4] D W Zuo and H X Jia, *Optik* **127**, 11282 (2016)
- [5] D W Zuo, *Appl. Math. Lett.* **79**, 182 (2018)
- [6] X Y Wen and Y Chen, *Pramana – J. Phys.* **91**: 23 (2018)
- [7] X Y Wen, Z Y Yan and Y Q Yang, *Chaos* **26**, 063123 (2016)
- [8] X Y Wen and Z Y Yan, *Commun. Nonlinear Sci. Numer. Simul.* **43**, 311 (2017)
- [9] X Y Wen, Y Q Yang and Z Y Yan, *Phys. Rev. E* **92**, 012917 (2015)

- [10] X Y Wen and Z Y Yan, *Chaos* **25**, 123115 (2015)
- [11] X Y Wen and G Q Zhang, *Mod. Phys. Lett. B* **32**, 1850005 (2018)
- [12] G Z Tu, *J. Phys. A* **23**, 3903 (1990)
- [13] M Toda, *Theory of nonlinear lattices* (Springer, Berlin, 1989)
- [14] M Wadati, *Prog. Theor. Phys. Suppl.* **59**, 36 (1977)
- [15] D J Kaup, *Math. Comput. Simul.* **69**, 322 (2005)
- [16] R Hirota, *J. Phys. Soc. Jpn* **35**, 289 (1973)
- [17] M J Ablowitz and P A Clarkson, *Solitons, nonlinear evolution equations and inverse scattering* (Cambridge University Press, New York, 1991)
- [18] M J Ablowitz and H Segur, *Solitons and the inverse scattering transform* (SIAM, Philadelphia, 1981)
- [19] M J Ablowitz and F J Ladik, *Stud. Appl. Math.* **55**, 213 (1976)
- [20] R Hirota and J Satsuma, *Prog. Theor. Phys. Suppl.* **59**, 64 (1976)
- [21] X G Geng, H H Dai and C W Cao, *J. Math. Phys.* **44**, 4573 (2003)
- [22] V B Matveev and M A Salle, *Darboux transformations and solitons* (Springer-Verlag, Berlin, 1991)
- [23] N Liu and X Y Wen, *Mod. Phys. Lett. B* **32**, 1850085 (2018)
- [24] L Liu, D S Wang, K Han and X Y Wen, *Commun. Nonlinear Sci. Numer. Simul.* **63**, 57 (2018)
- [25] X Y Wen, *Rep. Math. Phys.* **71**, 15 (2013)
- [26] H Q Zhao, Z N Zhu and J L Zhang, *Commun. Theor. Phys.* **56**, 23 (2011)
- [27] X Y Wen, *Appl. Math. Comput.* **218**, 5796 (2012)
- [28] X Y Wen, Z Y Yan and B A Malomed, *Chaos* **26**, 123110 (2016)
- [29] X Y Wen, *E. Asian J. Appl. Math.* **8**, 100 (2018)
- [30] R Guo, J Y Song, H T Zhang and F H Qi, *Mod. Phys. Lett. B* **32**, 1850152 (2018)
- [31] X Y Wen and D S Wang, *Wave Motion* **79**, 84 (2018)
- [32] X Y Wen, X H Meng, X G Xu and J T Wang, *Appl. Math. Lett.* **26**, 1076 (2013)
- [33] Y T Wu and X G Geng, *J. Phys. A* **31**, 677 (1998)
- [34] F J Yu and S Feng, *Math. Methods Appl. Sci.* **40**, 5515 (2017)
- [35] X X Xu, *Commun. Nonlinear Sci. Numer. Simul.* **23**, 192 (2015)
- [36] X X Xu and Y P Sun, *J. Nonlinear Sci. Appl.* **10**, 3328 (2017)
- [37] S Y Lou, B Tong, M Jia and J H Li, e-print arXiv:0711.0420 (2007)
- [38] J H He and X H Wu, *Chaos Solitons Fractals* **241**, 700 (2006)
- [39] P Liu and S Y Lou, *Chin. Phys. Lett.* **27**, 020202 (2010)
- [40] M J Ablowitz and J F Ladik, *Stud. Appl. Math.* **57**, 1 (1977)
- [41] R Sahadevan and S Balakrishnan, *J. Math. Phys.* **49**, 113510 (2008)
- [42] H Q Zhao, Z N Zhu and J L Zhang, *Chin. Phys. Lett.* **28**, 050202 (2011)
- [43] H Q Zhao and Z N Zhu, *J. Math. Phys.* **52**, 023512 (2011)
- [44] J K Yang, *Nonlinear waves in integrable and nonintegrable systems* (SIAM, Philadelphia, 2010)
- [45] L Lee, G Lyng and I Vankova, *Physica D* **241**, 1767 (2012)